Макрогетероциклы
http://macroheterocycles.isuct.ru

DOI: 10.6060/mhc171141n

Porphyrins Encapsulated into Pluronic F127 Micelles: Evaluating the Effect of the Central Metal and Substituents on the Photophysicochemical Properties in Water

Muthumuni Managa and Tebello Nyokong[@]

Dedicated to professor Aslan Yu. Tsivadze on the occasion of his Birthday

Centre for Nanotechnology Innovation, Department of Chemistry, Rhodes University, 6140 Grahamstown, South Africa
[@]Corresponding author E-mail: t.nyokong@ru.ac.za

*Metal free 5-(4-carboxyphenyl)-10,15,20-tris(phenyl)porphyrin (**1-H$_2$**) and its ClGa derivative (**1-ClGa**), as well as metal free 5-(4-(4-carboxyphenoxy)phenyl)-10,15,20-tris(phenyl)porphyrin (**2-H$_2$**) and its ClGa (**2-ClGa**), Zn (**2-Zn**) and Cl$_2$Si (**2-Cl$_2$Si**) derivatives were encapsulated into Pluronic F127 micelles to form **1-H$_2$**+F127, **2-H$_2$**+F127, **2-ClGa**+F127, **2-Zn**+F127 and **2-Cl$_2$Si**+F127. The fluorescence and singlet oxygen generating behaviour of the porphyrins were also investigated. The Stern-Volmer constant (K$_{sv}$) for **2-Zn**+F127 was the highest compared to other porphyrin derivatives.*

Keywords: Carboxy porphyrins, singlet oxygen quantum yield, fluorescence quenching, Pluronic F127 micelles.

Порфирины, инкапсулированные в мицеллы Pluronic F127: оценка влияния центрального металла и заместителей на фотофизико–химические свойства в воде

М. Манага, Т. Ниоконг[@]

Центр инноваций в области нанотехнологии, кафедра химии, Университет Родса, 6140 Грахамстаун, ЮАР
[@]E-mail: t.nyokong@ru.ac.za

*5-(4-Карбоксифенил)-10,15,20-трис(фенил)порфирин (**1-H$_2$**) и его ClGa комплекс (**1-ClGa**), а также 5-(4-(4-карбоксифенокси)фенил)-10,15,20-трис(фенил)порфирин (**2-H$_2$**) и его ClGa (**2-ClGa**), Zn (**2-Zn**), Cl$_2$Si (**2-Cl$_2$Si**) производные были инкапсулированы в мицеллы Pluronic F127 с образованием **1-H$_2$**+F127, **2-H$_2$**+F127, **2-ClGa**+F127, **2-Zn**+F127 и **2-Cl$_2$Si**+F127. Также были исследованы флуоресценция и образование синглетного кислорода порфиринов. Константа Штерна-Фольмера (K$_{sv}$) для **2-Zn**+F127 была самой высокой по сравнению с другими производными порфиринов.*

Ключевые слова: Карбоксипорфирины, квантовый выход синглетного кислорода, флуоресцентное тушение, мицеллы Pluronic F127.

Introduction

Polymer micelles are fast becoming a powerful nanomedicine platform for cancer therapeutic applications because of their biocompatibility and relatively small size (10–100 nm) which help to prevent them from being recognized by proteins and macrophages therefore allowing for a greater circulation time.[1] Polymer micelles also have the ability to solubilize water insoluble anticancer drugs such as porphyrins which are a subject of the current work.[2]

The polymeric micelles of interest in this work are the Pluronic triblock copolymers which are composed of poly(ethylene oxide) (PEO) and poly(propylene oxide) (PPO) with a PEO-PPO-PEO structure (Scheme 1).[3] The PEO and PPO segments on the micelles act, respectively, as hydrophilic corona and hydrophobic core.[3] Due to their biocompatibility and high drug loading ability, several Pluronics have been approved by Food and Drug Administration (FDA) for oral or intravenous administration because they are widely employed as solubilizers, emulsifiers or coating agents.[1,4-6]

Porphyrins have poor solubility[7] and are also known to aggregate,[8] which affects their photophysical behaviour. The driving forces behind the aggregation of porphyrins are the cooperative formation of hydrogen bonds, van-der-Waals forces and the hydrophobic effects.[9-11] Pluronic micelles reduce self-aggregation and increase solubility of porphyrins in aqueous media.[9,12]

The porphyrins employed in this work are: metal free 5-(4-carboxyphenyl)-10,15,20-*tris*(phenyl)porphyrin (**1-H_2**) and its ClGa derivative (complex **1-ClGa**) as well as metal free 5-(4-(4-carboxyphenoxy)phenyl)-10,15,20-*tris*(phenyl) porphyrin (**2-H_2**) and its ClGa, Zn and Cl_2Si derivatives (**2-ClGa**, **2-Zn**, and **2-Cl_2Si**, respectively), Figure 1. The heavy Ga and Zn central metals as well as the chloride axial ligands for Ga and Si derivatives employed in this work will result in improved intersystem crossing to the triplet state due to the heavy atom effect, and subsequently increase singlet oxygen generation which is essential for PDT. This work reports for the first time on the encapsulation of complexes **1** and **2** onto Pluronic F127 which could expand and improve on areas of PDT applications. Complexes **2** have been linked to Pluronic-silica nanoparticles for PDT applications in organic media.[13] In this work these complexes are embedded in Pluronic 127 micelles for the first time. Study of porphyrins in aqueous media is essential for applications in biological systems such as in PDT.

Porphyrins which are *meso*-phenyl substituted with carboxy functional groups have been reported as efficient second generation photosensitizers for PDT,[14] hence complexes **1** and **2** are employed in this work.

Experimental

Materials

Pluronic F127 (MW ~12.600 g/mol), potassium iodide, 9,10-anthracenediyl-*bis*(methylene)dimalonic acid (ADMA), metal free tetrakis(4-sulfonatophenyl)porphyrin (H_2TSPP), and Zn tetraphenylporphyrin (ZnTPP) were purchased from Sigma-Aldrich. Dichloromethane (DCM) and dimethylformamide (DMF) were purchased from Merck. All other reagents and solvents were obtained from commercial suppliers and used as received. The syntheses of metal free 5-(4-carboxyphenyl)-10,15,20-*tris*(phenyl) porphyrin (**1-H_2**) and its ClGa derivative (**1-ClGa**),[15] and metal free 5-(4-(4-carboxyphenoxy)phenyl)-10,15,20-*tris*(phenyl)porphyrin (**2-H_2**) and its ClGa, Zn and Si derivatives (**2-ClGa**, **2-Zn**, **2-Cl_2Si**),[13] Figure 1, have been reported.

Equipment

Ground state electronic absorption spectra were recorded at room temperature using on a Shimadzu UV-2550 spectrophotometer and a 1 cm pathlength cuvette. Dynamic light scattering (DLS) experiments were done on a Malvern Zetasizer nanoseries, Nano-ZS90. Fluorescence emission spectra were recorded on a Varian Eclipse spectrofluorometer. Fluorescence lifetimes were measured using a time correlated single photon counting setup (TCSPC) (FluoTime 300, Picoquant GmbH) with a diode laser (excitation source: LDH-P-485 with 10 MHz repetition rate, 88 ps pulse width). Details have been provided before.[16]

Photo-irradiations for singlet oxygen studies in water (in the presence of micelles) were done using a General Electric projector lamp (300 W). A water filter was used to filter off infrared radiations. Light intensities were measured with a POWER MAX5100 (Molelectron detector incorporated) power meter. This means irradiation encompassed both the *Q* and Soret bands. Light intensity was determined to be $9.43 \cdot 10^{18}$·photons $s^{-1} \cdot cm^{-2}$. Background studies were performed to determine if ADMA degrades in the absence of porphyrins. Irradiation of ADMA was done under the same irradiation intensity and time used for singlet oxygen studies.

Fluorescence quantum yield

Fluorescence quantum yields (Φ_F) were determined by comparative methods,[17] Equation (1), using the fluorescence quantum yield of ZnTPP in DMF as a standard (Φ_F^{Std}) = 0.033.[18]

$$\Phi_F = \Phi_F^{Std} \frac{F\, A^{Std}\, n^2}{F^{Std} A\, (n^{Std})^2}, \quad (1)$$

where F and F^{Std} are the areas under the fluorescence curves for sample and standard, respectively. A and A^{Std} are the absorbances of the sample and reference at the excitation wavelength, respectively. n and n_{Std} are the refractive indices of the solvent used for the sample and standard, respectively. Absorbance at the excitation wavelength was ~0.05 in order to minimize inner filter effects. At least three independent experiments were performed for the quantum yield determinations. Both the sample and the standard were excited at the same relevant wavelength.

Singlet oxygen quantum yield (Φ_Δ)

Singlet oxygen quantum yield values in water were determined under ambient conditions using the chemical method with ADMA as a singlet oxygen quencher in water using Equation (2).[19]

$$\Phi_\Delta = \Phi_\Delta^{Std} \frac{W\, I_{abs}^{Std}}{W^{Std} I_{abs}}, \quad (2)$$

where Φ_Δ^{Std} is the singlet oxygen quantum yield for the standard (H_2TSPP) in water (=0.51),[20] W and W^{Std} are the ADMA photobleaching rates in the presence of porphyrin derivatives under investigation and the standard, respectively. I_{abs} and I_{abs}^{Std} are the rates of light absorption by the porphyrin derivative and standard, respectively.

I_{abs} is determined by Equation (3).

$$I_{abs} = \frac{\alpha S I}{N_A}, \quad (3)$$

where α is the fraction of light absorbed, S is the cell area irradiated, N_A is Avogadro's constant and *I* the light intensity. The absorbances used for Equation (3) are those of the porphyrins embedded in micelles. The light intensity measured refers to the light reaching the spectrophotometer cells and it is expected that some of the light may be scattered since the system is heterogeneous. In addition, the wavelength employed covers a wide range, hence the Φ_Δ values of the porphyrins in the micelles are estimates and used for comparison only.

Incorporation of porphyrins into Pluronic F127

The incorporation of all porphyrins (structures shown in Figure 1) into micelles was carried out using the solid dispersion method which has been described in literature.[21,22] This method involves cosolubilization of copolymer with the porphyrin, which is then followed by rotative evaporation as follows: **1-H_2** ($7.22\cdot10^{-4}$ M), **1-ClGa** ($6.57\cdot10^{-4}$ M), **2-H_2** ($6.66\cdot10^{-4}$ M), **2-ClGa** ($5.85\cdot10^{-4}$ M), **2-Zn** ($5.92\cdot10^{-4}$ M) and **2-Cl_2Si** ($6.15\cdot10^{-4}$ M) were each mixed with Pluronic F127 (20 % w/V, $1.5\cdot10^{-2}$ M) in 10 mL DCM. The mixtures were sonicated for 15 min at room temperature. The solvent was then removed using the rotary evaporator. The achieved solid products were left in a vacuum desiccator for 12 h and then hydrated and vigorously stirred (Dubnoff metabolic shaking) at 70 °C for 4 h. The solutions were transferred onto test tubes and left for 24 h undisturbed for precipitation of porphyrins which were not bound onto the polymer which were then filtered and the required product was dried. The porphyrins when loaded into Pluronic F127 are represented as **1-H_2**+F127, **1-ClGa**+F127, **2-H_2**+F127, **2-ClGa**+F127, **2-Zn**+F127 and **2-Cl_2Si** +F127.

Fluorescence quenching

For these studies, stock solutions ($1.0\cdot10^{-6}$ M) based on the Soret band absorption peak of the porphyrin with the micelles of **1-H_2**+F127, **1-ClGa**+F127, **2-H_2**+F127, **2-ClGa**+F127, **2-Zn**+F127 and **2-Cl_2Si**+F127 were prepared. Solutions of I^- with different concentrations of 0 M to 0.6 M in water were also prepared. For the quenching experiments, 2.5 mL of the porphyrin-micelles and 500 µL of different concentrations of I^- were mixed (a total volume of 3 mL each time) and allowed to equilibrate for 5 min before fluorescence measurement were taken. Thus, the concentration of the porphyrin-micelles was kept constant while that of I^- was varied. The actual concentration of I^- in the mixture is employed for the calculations of the Stern-Volmer constants.

Results and Discussion

Characterization of porphyrins when embedded in Pluronic F127

The structures of the porphyrins employed are shown in Figure 1. The incorporation of all porphyrins into micelles was carried out using the solid dispersion method which has been described in literature[21,22] as stated above. The porphyrins become water soluble after incorporation into Pluronic F127 micelles, hence all the studies are done in water in this work. No comparison can be made between porphyrins alone

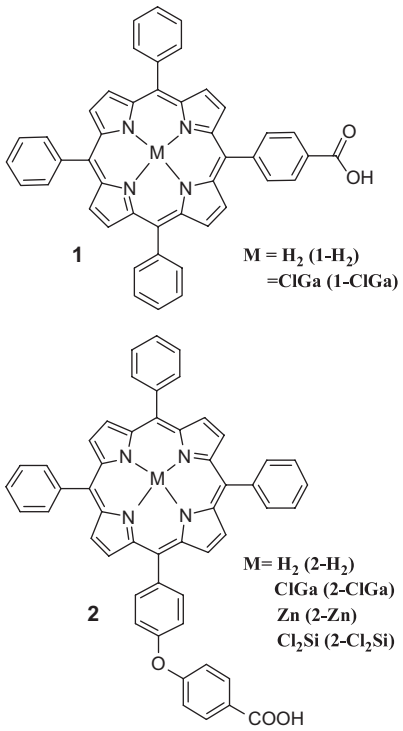

Figure 1. Structures of the porphyrins employed.

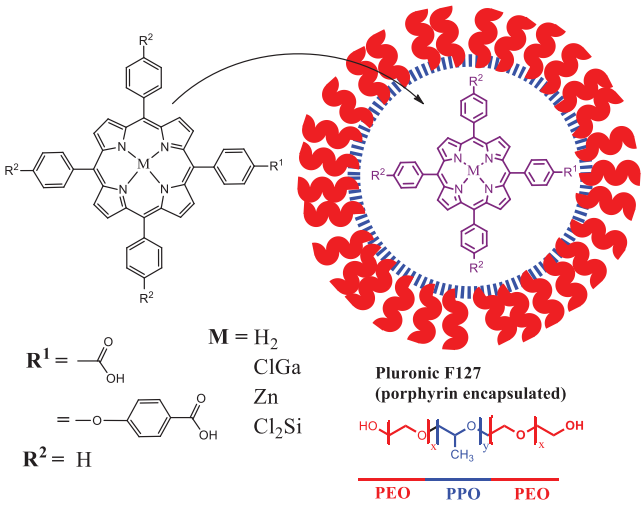

Scheme 1. Incorporation of the porphyrins into Pluronic F127.

dissolved in organic solvents and when they are embedded in micelles since different solvents are used. Also comparison with carboxylic acid porphyrins linked to Pluronic silica nanoparticles[13] or linked to δ-aminolevulinic acid[15] is not possible since the reported work was done in organic media while this work is done on porphyrins is aqueous media.

UV-Vis spectra

The ground state electronic absorption spectra of porphyrins are characterized by an intense band called the Soret or B band at around 400 nm. The Soret bands were observed at 418 nm, 423 nm for **1-H_2**+F127 and **1-ClGa**+F127, respectively. While the Soret bands of **2-H_2**+F127, **2-ClGa**+F127,

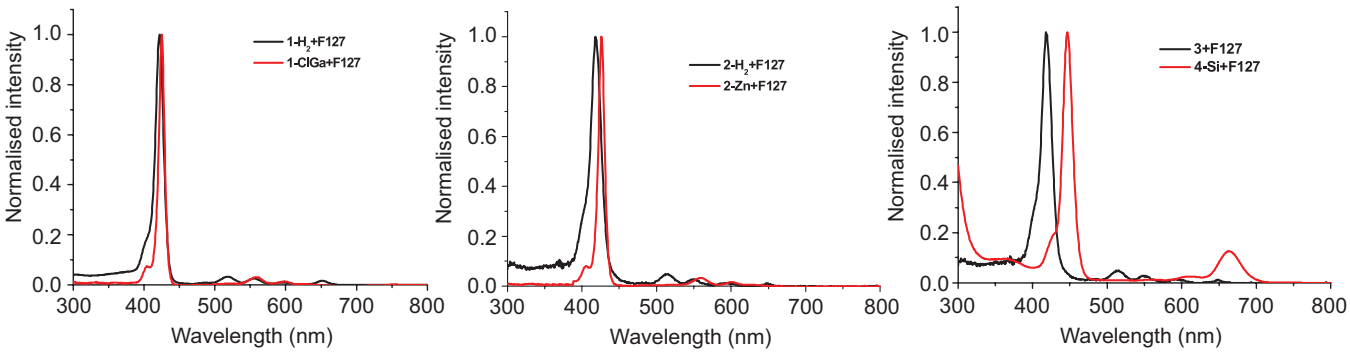

Figure 2. Normalised electronic absorption spectra of porphyrin when loaded in Pluronic F127 in water.

2-Zn+F127 and **2-Cl$_2$Si** +F127 were observed at 419 nm, 423 nm, 426 nm and 446 nm, respectively (Table 1). The four *Q*-bands of the metal free porphyrins collapsed into two *Q*-bands for the metalated derivatives (Figure 2). There are red shifts in the Soret bands upon introduction of central metals for all porphyrins. Introduction of heavy metals results in degree of perturbation and electron delocalisation within the porphyrin macrocycle.[23] In addition, red-shifts of Soret bands are often observed for distorted porphyrins.[24] Comparing **2-H$_2$**+F127, **2-ClGa**+F127, **2-Zn**+F127 and **2-Cl$_2$Si**+F127; the latter (**2-Cl$_2$Si**+F127) has a more red shifted Soret band. Broad and red shifted Soret band may also indicate *J*-aggregation of porphyrins.[25] However, there is no clear broadening in Figure 2 for **2-Cl$_2$Si** +F127 even though there is more red-shifting for this conjugate compared to **2-ClGa**+F127 and **2-Zn**+F127. In order to check the effect of the substituent on the spectra, conjugates **1-ClGa**+F127 and **2-ClGa** +F127 containing the same central metal and different substituents were compared, but there was no shift in the Soret peak maxima, showing no substituent effect. The same applies when comparing **1-H$_2$**+F127 and **2-H$_2$**+F127, both metal free but containing different substituents.

After the determination of the ε values of porphyrins in F127 aqueous solutions, the relationships between the photosensitizer incorporation capacity and the concentration were evaluated. The actual amounts of porphyrins embedded into micelles were determined from ε values using the Beer-Lambert law and maximum absorbance of the *Q* bands following reported methods.[26] The values are that were determined to be 0.077, 0.071, 0.075, 0.011, 0.036 and 0.055 mg of **1-H$_2$**+F127, **1-ClGa**+F127, **2**+F127, **2-ClGa**+F127, **2-Zn**+F127 and **2-Cl$_2$Si** +F127, respectively, hence the highest loading is that of **1-H$_2$**+F127, Table 1.

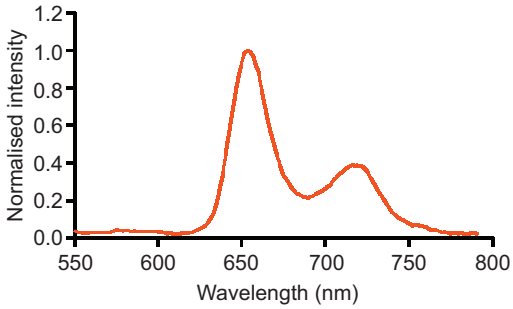

Figure 3. Fluorescence emission spectrum of **1-H$_2$**+F127 in water.

Figure 3 shows the emission spectra of **1-H$_2$**+F127 as an example. The spectra are typical[27] of porphyrins with two bands differing in intensity. Very weak emission signals were obtained for the rest of the conjugates due to the presence of heavy central metals and/or chlorine which will result in intersystem crossing to the triplet state hence quenching fluorescence.

Dynamic light scattering (DLS)

The micelle sizes were determined using dynamic light scattering (DLS). The size of Pluronic F127 has been previously been reported to be 14.6 nm.[21] The sizes of the porphyrin containing micelles were determined

Table 1. The photophysical properties of porphyrins embedded in Pluronic F127 in water.

Conjugates[a]	Amount of porphyrin loaded (mg)	λ_{Abs} [b] (nm)	λ_{Em} [b] (nm)	Φ_F	τ_F (ns)	Φ_Δ(±0.01)	K_{sv} (M^{-1})
1-H$_2$+F127 (15.65)	0.077	418	655, 719	0.10	4.63	0.29	0.26
1-ClGa+F127 (30.91)	0.071	423	615, 654	<0.01	3.20	0.31	1.79
2-H$_2$+F127 (16.35)	0.075	419	657, 720	0.11	4.06	0.32	0.35
2-ClGa+F127 (33.57)	0.011	423	615, 657	<0.01	3.11	0.37	2.18
2-Zn+F127 (32.71)	0.036	426	620, 655	<0.01	3.01	0.35	2.27
2-Cl$_2$Si +F127 (31.87)	0.055	446	652, 699	<0.01	3.23	0.34	1.91

[a]Values in brackets are the sizes determined by DLS in brackets. [b]λ_{Abs}=absorption, λ_{Em}=emission.

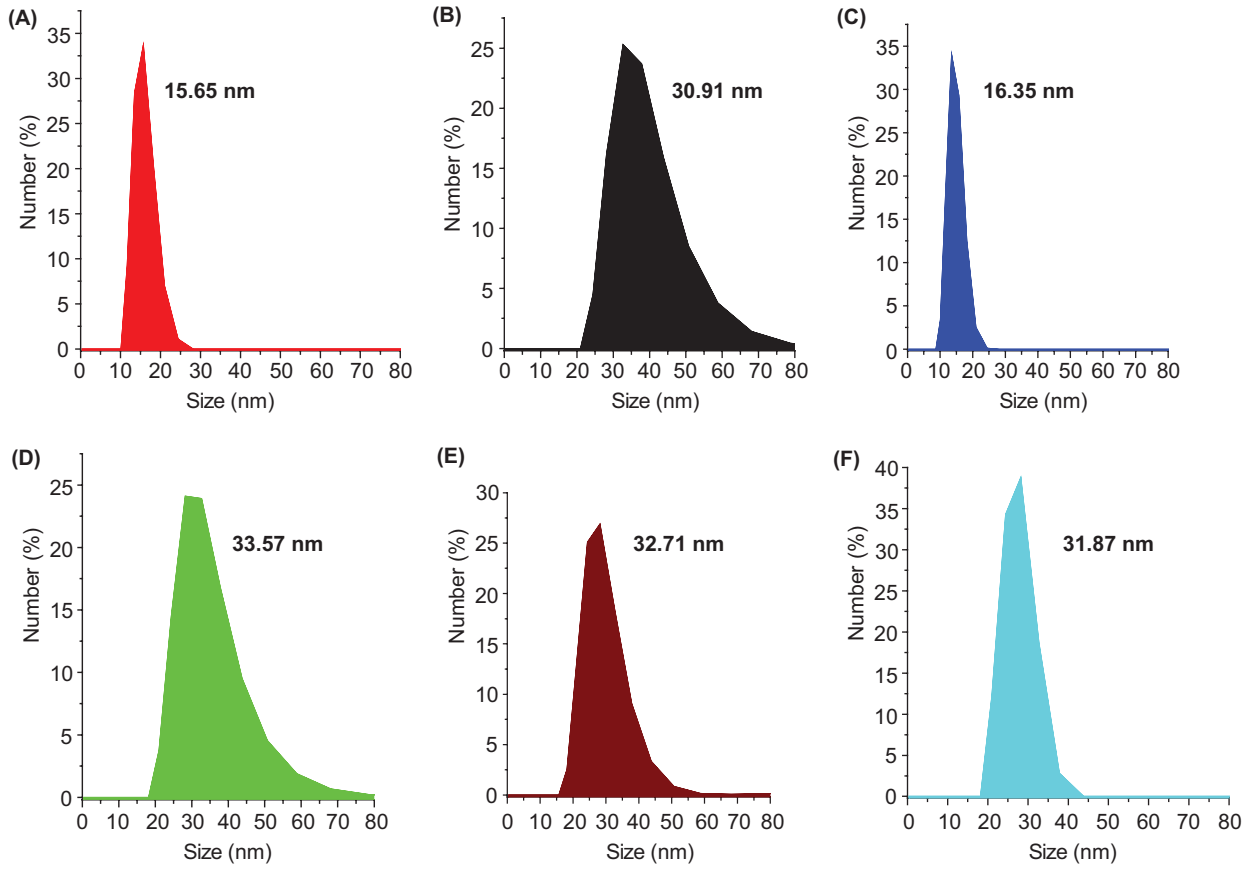

Figure 4. Dynamic light scattering of micelles containing porphyrins: (A) **1-H$_2$**+F127, (B) **1-ClGa**+F127, (C) **2-H$_2$**+F127, (D) **2-ClGa**+F127, (E) **2-Zn**+F127 and (F) **2-Cl$_2$Si**.

to be 15.65 nm, 30.91 nm, 16.35 nm, 33.57 nm, 32.71 nm and 31.87 nm for **1-H$_2$**+F127, **1-ClGa**+F127, **2-H$_2$**+F127, **2-ClGa**+F127, **2-Zn**+F127 and **2-Cl$_2$Si**+F127, respectively, Table 1. In all cases (Table 1 and Figure 4), metal free conjugates have smaller sizes as compared to the corresponding metalated derivatives. It has been reported that central metals within the cavity of the porphyrins change the hydrophobicity of the molecule.[28] It was also found that the most hydrophobic drugs increased the sizes of the micellar core and corona,[29] hence the increase in size of micelles containing metalated porphyrins compared to metal free ones could be a result of increased hydrophobicity of the former, while small differences in sizes for the micelles of metalated derivatives reflect small differences in hydrophobicity.

Fluorescence quantum yields (Φ_F) and lifetimes (τ_f)

The florescence quantum yields (Φ_F) were determined using a comparative method and exciting at 490 nm. The Φ_F of **1-H$_2$**+F127 and **2-H$_2$**+F127 were determined to be 0.10 and 0.11, respectively, while those of **1-ClGa**+F127, **2-ClGa**+F127, **2-Zn**+F127 and **2-Cl$_2$Si**+F127 were all determined to be <0.01. The values in the presence of ClGa and Zn and Cl$_2$Si are low due to the heavy atom effects of central metals and axial ligands, which results in intersystem crossing to the triplet state, reducing fluorescence.

The fluorescence life-time (τ_f) values for **1-H$_2$**+F127, **1-ClGa**+F127, **2-H$_2$**+F127, **2-ClGa**+F127, **2-Zn**+F127 and **2-Cl$_2$Si**+F127 were determined using a time correlated single photon count (TCSPC) method, following excitation at the emission maxima. A typical fluorescence decay profile for of **2-Zn**+F127 as an example is shown in Figure 5. Mono-exponential decay profiles were obtained for all porphyrin complexes. The τ_f values follow the trend of Φ_F since there is a decrease on metalation.

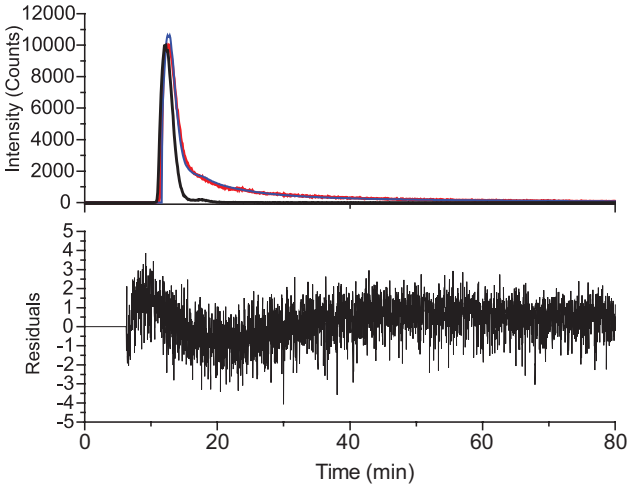

Figure 5. Fluorescence decay profile of **2-Zn**+F127 as an example in water. Black line represents the instrument response function (IRF), blue line is the data and red line is the fitting.

Singlet oxygen quantum yield (Φ_Δ)

The metal free porphyrins generally have lower Φ_Δ compared to metalated porphyrins, Table 1. ADMA was employed as a singlet oxygen quencher. As stated above, these values are estimates for comparison purposes only. Since the light used for singlet oxygen studies covered the range where ADMA absorbs, the effect of light on ADMA alone was investigated. There was no significant decrease in the absorbance of ADMA within the time scale used for singlet oxygen quantum yield studies. The values in the presence of ClGa, Zn and Cl_2Si are high due to the heavy atom effect of the central metals and axial Cl^- ligands which results in intersystem crossing to the triplet state from which singlet oxygen is generated as previously mentioned. It has been reported in literature[30] that an increase in Φ_Δ values is expected when porphyrins are incorporated into Pluronic polymers, however the results previously reported are incomparable as they were carried out in DMF.[13,15] According to literature,[8] the PEO segment of the polymer may hinder collision of the porphyrin with surrounding molecules thus obstructing idle losses of the triplet state energy therefore increasing Φ_Δ. Comparing **1-H$_2$**+F127 with **2-H$_2$**+F127 both metal free, but containing different substituents shows that the latter gave larger Φ_Δ value. Again, the same applies when comparing **1-ClGa**+F127 with **2-ClGa**+F127, both containing the same Ga central metal but different substituents, showing the effects of the bulkier phenoxy benzoic acid substituent. Comparing **2-ClGa**+F127, **2-Zn**+F127 and **2-Cl$_2$Si**+F127 shows that **2-ClGa**+F127 gave the largest Φ_Δ value, showing the combined heavy atom effects of Ga and the Cl^- axial ligand, though the effect is not too large. The higher loading for **1-H$_2$**+F127 could have also resulted in aggregation, hence the lowest Φ_Δ value.

Determination of Stern-Volmer constants

The relative locations of porphyrins in Pluronic F127 micellar system were carried out by fluorescence quenching. I^- was employed as a quencher. Stern-Volmer constants (K_{sv}) were calculated using Equation (4):

$$\frac{F_0}{F} = 1 + K_{SV}[Q], \quad (4)$$

where F_0 and F are the fluorescence intensities in the absence and presence of the quencher, respectively, [Q] is the concentration of the quencher.

Figure 6A-B shows the fluorescence quenching spectra from which Stern-Volmer plots were derived. The Stern–Volmer plots (inserts (a)) showed nonlinear relationships. These types of plots can occur in the case of purely collisional quenching but with some of the fluorophores being less accessible than others.[31,32] Inserts (a) in Figure 6 A-B are a characteristic feature of two fluorophore populations. Some porphyrins are buried in the polymer interior and are relatively inaccessible to iodide while the others are on the polymer surface and are more accessible.[31]

The deviation from linearity in the Stern-Volmer plots is accommodated by treating the data using a modified Stern-Volmer equation by Sam Lehrer Eq. (5) which takes into account situations where two populations of fluorophores exist, with one being accessible to quencher and the other being buried and not accessible.[33]

$$\frac{F_0}{\Delta F} = \frac{1}{([Q] f_a K_{SV})} + \frac{1}{f_a}, \quad (5)$$

where F_0 is the fluorescence intensity in the absence of quencher, ΔF is the observed decrease in the fluorescence and K_{sv} is the Stern-Volmer quenching constant of the accessible fluorophore. f_a is the fluorescence of the fluorophore which is accessible to the quenchers (Q). Plots of $F_0/\Delta F$ *versus* 1/[Q] with an Y-axis intercept of $1/f_a$ are shown in Figure 6 A-B (inserts (b)).

A low K_{sv} value indicates that dyes are located in the micelle core, resulting in less encounter between incorporated photosensitizer and iodine.[33,34] The K_{sv} values obtained for **1-H$_2$**+F127 was 0.26 M^{-1} and was 1.79 M^{-1} for **1-ClGa**+F127. The K_{sv} **2**+F127, **2-ClGa**+F127, **2-Zn**+F127 and **2-Cl$_2$Si**+F127 were determined to be 0.35, 2.18, 2.27 and 1.91 M^{-1}. Thus, **2-Zn**+F127 is located more on

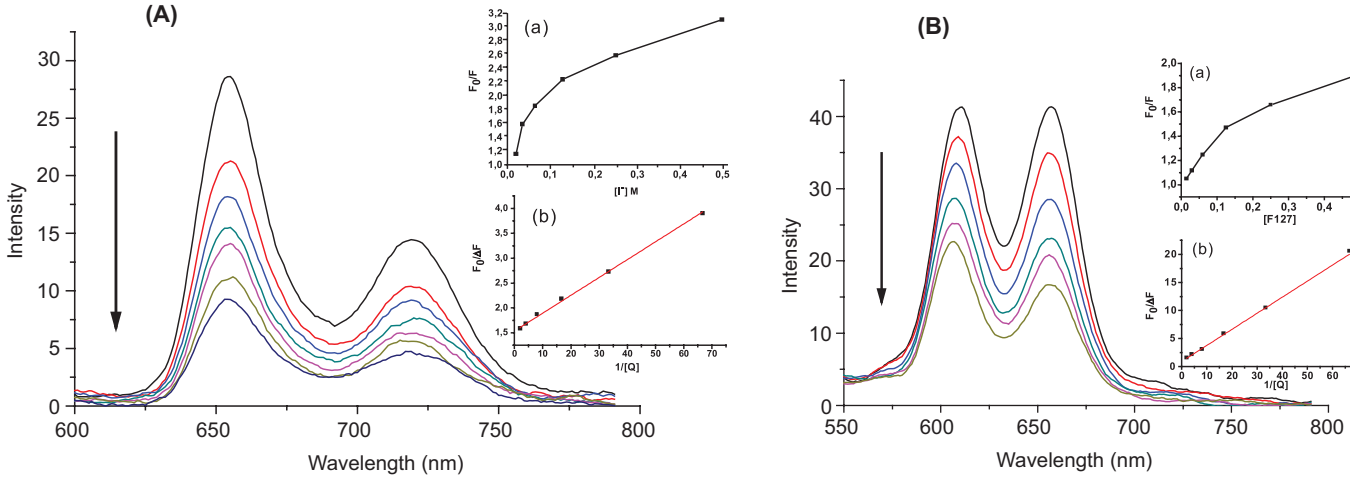

Figure 6. Fluorescence emission spectra for (A) **2-H$_2$**+F127 and (B) **2-Zn**+F127 (as examples) in the presence of 0 M to 0.10 M of KI. Excitation wavelength=490 nm. Inserts: (a) Stern-Volmer plot using Equation 4 and (b) modified Stern-Volmer plot using Equation 5.

the hydrophilic outer area (and can interact with the quencher more) than the corresponding **2-H_2**+F127, **2-ClGa**+F127, and **2-Cl_2Si**+F127 since the former has a larger K_{sv} value. As stated above, metals in the centre of porphyrins changes the hydrophobicity of the molecule therefore resulting in the different locations for the porphyrins. Metal free derivatives **1-H_2**+F127 and **2-H_2**+F127 are located more in the hydrophobic inner core since they have the lower K_{sv} values compared to the corresponding metalated derivatives. Comparing **2-ClGa**+F127, **2-Zn**+F127 and **2-Cl_2Si** +F127 differing only in the central metal, the Cl_2Si derivative is located more in the hydrophobic inner core (smaller K_{sv} value) probably due to the smaller size, while the largest Zn derivative is located more on the outer hydrophilic core (larger K_{sv} value).

Conclusions

Metal free 5-(4-carboxyphenyl)-10,15,20-*tris*(phenyl) porphyrin) and its ClGa derivative as well as metal free 5-(4-(4-carboxyphenoxy)phenyl)-10,15,20-*tris*(phenyl) porphyrin and its ClGa, Zn and Cl_2Si derivatives were successfully encapsulated into Pluronic F127 micelles and upon encapsulation the porphyrins became water soluble which is ideal for biological application. The photophysical and fluorescence quenching studies were carried in water. It can be concluded out of all these complexes, complex **2-ClGa**+F127 showed better properties hence it can be effective in possible application for PDT.

Acknowledgements. This work was supported by the Department of Science and Technology (DST)/Nanotechnology (NIC) and National Research Foundation (NRF) of South Africa through DST/NRF South African Research Chairs Initiative for Professor of Medicinal Chemistry and Nanotechnology (UID 62620) and Rhodes University.

References

1. Vilsinski B.H., Gerola A.P., Enumo J.A., da Silva Souza Campanholi K., de Souza Pereira P.C., Braga G., Hiok N., Kimura E., Tessaro A.L., Caetano W. *Photochem. Photobiol*. **2015**, *91*, 518–525.
2. Sutton D., Nasongkla N., Blanco E., Gao J. *Pharm. Res.* **2007**, *24*, 1029–1046.
3. Kedar U., Phutane P., Shidhaye S., Kadam V. *Nanomedicine: NBM* **2010**, *6*, 714–729.
4. Sobczynski J., Kristensen S., Ber S. *Photochem. Photobiol. Sci.* **2014**, *13*, 8–22.
5. Alakhov V., Klinski E., Li S., Pietrzynski G., Venne A., Batrakova E.V., Bronitch T., Kabanov A.V. *Colloids Surf, B: Biointerfaces* **1999**, *16*, 113–34.
6. Zhang W., Shi Y., Chen Y., Ye J., Sha X., Fang X. *Biomaterials* **2011**, *32*, 2894–2906.
7. Sezgin Z., Yu¨ksel N., Baykara T. *Eur. J. Pharm. Biopharm*. **2006**, *64*, 261–268.
8. Kano K., Fukuda K., Wakami H., Nishiyabu R., Pasternack R.F. *J. Am. Chem. Soc.* **2000**, *122*, 7494–7502.
9. Whitesides G.M., Mathias J.P., Seto C.T. *Science* **1991**, *254*, 1312–1319.
10. Tozoni J.R., Barbosa N.M., Neto C.A., Ribeiro W.M., Pazin A., Ito S., Borissevitch I.E., Marletta A. *Polymer* **2016**, *102*, 136–142.
11. Sigge U., Bindig U., Endisch C., Komatsu T., Tsuchida E., Voigt J., Fuhrhop J.H. *Ber. Bunsen-Ges. Phys. Chem.* **2010**, *100*, 2070–2075.
12. Kwon G.S., Kataoka K. *Adv. Drug Delivery Rev.* **1995**, *16*(2-3), 295–309.
13. Managa M., Britton J., Prinsloo E., Nyokong T. *J. Coord. Chem*. **2016**, *69*, 3491–3506.
14. Bakar M.B., Oelgemoller M., Senge M.O. *Tetrahedron* **2009**, *65*, 7064–7078.
15. Managa M., Mkhize S., Britton J., Prinsloo E., Nyokong T. *J. Coord. Chem.* **2016**, *69*, 3035–3042.
16. Tshangana C., Nyokong T. *J. Fluoresc*. **2015**, *25*, 199–210.
17. Fery-Forgues S., Lavabre D. *J. Chem. Educ*. **1999**, *76*, 1260–1264.
18. Brookfield R.L., Ellul H., Harriman A., Porter G. *J. Chem. Soc., Faraday Trans*. **1986**, *82*, 219–233.
19. Kuznetsova N.A., Gretsova N.S., Yuzhakova O.A., Negrimovskii V.M., Kaliya O.L., Luk'yanets E.A. *Russ. J. Gen. Chem.* **2001**, *71*, 36–44.
20. Tanielian C., Wolff C., Esch M. *J. Phys. Chem.* **1996**, *100*, 6555–60.
21. Managa M., Ngoy B.P, Mafukidze D., Britton J., Nyokong T. *J. Photochem. Photobiol. A: Chemistry* **2017**, *348*, 179–187.
22. Eloy J.O., Marchetti J.M. *Powder Technol.* **2014**, *253*, 98–106.
23. Ye X., Zhang J., Chen H., Wang X., Huang F. *Appl. Mater. Interfaces* **2014**, *6*, 5113−5121.
24. Takayama S.J., Ukpabi G., Murphy M.E.P., Mauk A.G. *PNAS* **2011**, *108*, 13071–13076.
25. Togashi D.M., Costa S.M.B., Sobral A.J.F.N., Gonsalves A.M.d'A.R. *J. Phys. Chem. B* **2004**, *108*, 11344–11356.
26. Vilsinski B.H., Aparicio J.L., de Souza Pereira P.C., Fávaro S.L., Campanholi K.S.S., Gerola A.P., Tessaro A.L., Hioka N., Caetano W. *Quim. Nova* **2014**, *37*(10), 1650–1656.
27. Uttamlal M., Holmes-Smith A.S. *Chem. Phys. Lett.* **2008**, *454*, 223–28.
28. Wenceslau A.C., Ferreira G.L.Q.C., Hioka N., Caetano W. *J. Porphyrins Phthalocyanines* **2015**, *19*, 1168–1176.
29. Basak R., Bandyopadhyay R. *Langmuir* **2013**, *29*, 4350−4356.
30. Kotov S.L., Timofeev V.A., Belkov G.V., Aksenov N.A., Soloviev A.B. *Micron* **2012**, *43*, 445–449.
31. Lakowicz J.R. *Principles of Fluorescence Spectroscopy* (3rd ed.). New York: Springer Science Business Media, LCC, **2006**.
32. Jameson D.M. *Introduction to Fluorescence*. United State: CRC Press, Taylor & Francis Group, **2014**.
33. Gu Z., Lei W., Shi W., Hao Q, Si W., Xia X., Wang F. *Spectrochim. Acta, Part A* **2014**, *132*, 316–68.
34. Pellosi D.S., Estevão B.M., Freitas C.F., Tsubone T.M., Caetano W., Hioka N. *Dyes Pigm.* **2013**, *99*, 705–712.

Received 09.11.2017
Accepted 11.12.2017